Applied Surface Science 310 (2014) 100–111

Contents lists available at ScienceDirect

Applied Surface Science

journal homepage: www.elsevier.com/locate/apsusc

Resist materials for proton beam writing: A review

J.A. van Kan [a,*], P. Malar [b], Y.H. Wang [a]

[a] Centre for Ion Beam Applications, Physics Department, 2 Science Drive 3, National University of Singapore, 117542 Singapore, Singapore
[b] Research Institute, SRM University, Kattankulathur, Chennai 603203, India

ARTICLE INFO

Article history:
Received 31 December 2013
Received in revised form 17 April 2014
Accepted 18 April 2014
Available online 26 April 2014

Keywords:
Proton beam writing
Resist materials
Ni electroplating

ABSTRACT

Proton beam writing (PBW) is a lithographic technique that has been developed since the mid 1990s, initially in Singapore followed by several groups around the world. MeV protons while penetrating materials will maintain a practically straight path. During the continued slowing down of a proton in material it will mainly interact with substrate electrons and transfer a small amount of energy to each electron, the induced secondary electrons will modify the molecular structure of resist within a few nanometers around the proton track. The recent demonstration of high aspect ratio sub 20 nm lithography in HSQ shows the potential of PBW. To explore the full capabilities of PBW, the understanding of the interaction of fast protons with different resist materials is important.

Here we give an update of the growing number of resist materials that have been evaluated for PBW. In particular we evaluate the exposure and development strategies for the most promising resist materials like PMMA, HSQ, SU-8 and AR-P and compare their characteristics with respect to properties such as contrast and sensitivity. Besides an updated literature survey we also present new findings on AR-P and PMGI resists. Since PBW is a direct write technology it is important to look for fast ways to replicate micro and nanostructures. In this respect we will discuss the suitability and performance of several resists for Ni electroplating for mold fabrication in nano imprint technologies. We will summarize with an overview of proton resist characteristics like sensitivity, contrast, aspect ratio and suitability for electroplating.

1. Introduction

Proton beams have been used in masked lithography since 1979 [1]. In early experiments Adesida [2] and Brenner et al. [3] used low energy (200 keV) and high energy (8 MeV) proton beams respectively for masked irradiation of PMMA resist materials. In this early work Adesida produced rather rough sub-100 nm features, whereas Brenner et al. produced very high aspect ratio structures featuring lateral dimensions of tens of microns. It took a long time before protons were used more seriously in lithographic experiments. More recently proton beam writing (PBW) was introduced as a direct-write lithography process developed at the Centre for Ion Beam Applications (CIBA), Department of Physics, National University of Singapore [4–6]. The proton beam writing technique relies on a precise beam scanning and control system that offers a simple yet flexible interface for the fabrication and design of micro- and nanostructures using focused protons with a spot size down to 20 nm [7].

In proton structuring of resist materials there are two main modes of exposure. The choice between masked- or focused beam exposure depends on the nature of the application. In both cases resist characteristics like sensitivity, contrast and nature of the resist (positive or negative tone) are crucial for the success of the lithographic task at hand. In the case of metallic mold fabrication the resist needs to be easily removable after Ni electroplating, limiting the choice of resist materials. Equally important is the fact that protons travel in a relatively straight path and the secondary electrons produced have limited range [8,9] allowing unique structuring of 3D nanostructures with high aspect ratios (height/width).

1.1. Exposure strategies

To facilitate high aspect ratio 3D nanostructuring of resist material, PBW using a focused beam has shown the most promising results. At CIBA Ionscan software is used to pattern resist materials in PBW experiments. The Ionscan software suite is comprised of sub programs to control beam scanning, beam blanking, stage movement and file conversion. The first version was developed using *LabVIEW* [10]. Many new features have since been added into the software, e.g. the ability to perform combined stage and beam scanning, resist calibration, dose calculation, scan parameters settings

* Corresponding author.
E-mail address: phyjavk@nus.edu.sg (J.A. van Kan).

http://dx.doi.org/10.1016/j.apsusc.2014.04.147
0169-4332/

and automated serial writing [11]. Every exposure pattern is digitized with a resolution up to 16 bit with a minimum pixel dwell time of 1 μs/pixel. The maximum beam scan area depends on the beamline used and is either 500 μm × 500 μm [5] or 100 μm × 100 μm [7] for the 1st and 2nd generation PBW systems respectively. In PBW experiments it is important to have a stable and reliable exposure system, and especially the proton source brightness and choice of the proton beam energy are important factors in achieving high quality high aspect ratio micro and nanostructures.

Several groups have used collimated proton beams for resist lithography with MeV protons. Tuteleers et al. [12,13] have introduced high energy (8–16.5 MeV) masked exposures for the production of optical components made from PMMA. At CIBA ion projection lithography of Si using molecular proton beams has been introduced by Mangaiyarkarasi et al. [14] to fabricate a variety of optical and photonic components in Si over wafer areas of several square centimetres. This process is based on a projection system involving a megavolt accelerator and a quadrupole lens system to project a uniform distribution of MeV ions over a wafer surface, which is coated with a multilevel mask. The features in the mask determine the resolution of the process. In conjunction with electrochemical anodization, this enables the rapid production of waveguides and optical microcavities for applications in high-definition reflective displays and optical communications.

As an alternative approach Puttaraksa et al. [15] introduced a programmable proximity aperture lithography (PPAL) technique. Using this PPAL technique they have made a large area microfluidic chip with complex components having large and small (1–500 μm) patterned elements on PMMA. After bonding the PMMA chips were used in fluidic environment. In this technique, a rectangular or square exposed area on the sample is adjustable and determined by two computer-controlled L-shaped aperture blades. A LABVIEW™ program controls the opening aperture area, the exposed sample position and the beam blanking. Complex structures can be built up by connecting several pattern elements with control up to 100 nm translational steps with 2 μm accuracy in bidirectional setting and 4 μm accuracy in absolute position. In the case of 3 MeV $^4He^{2+}$ ions, the exposure time used is approximately 45 s per pattern element corresponding to an ion fluence of 2.5×10^{13} ions/cm^2.

1.2. Technological challenges and proton interaction with resist

To achieve features below 10 nm using PBW several technological challenges need to be met. We have identified three main requirements:

Firstly: A lens system must be able to focus proton beams down to nm sized dimensions. The lens system developed in CIBA [7,16] is expected to be able to cross the 10 nm barrier.

Secondly: The proton source brightness in available PBW systems is currently very low and needs to be improved in order for PBW to become a viable contender in nanolithography. Novel ion source ideas are being evaluated at the moment [17].

Thirdly: A suitable resist material and development procedure need to be employed to realize sub 10 nm resist features. To explore the full micro- and nano-fabricating capabilities of protons in lithography, and PBW in particular it is important to understand the interaction of MeV protons with resist materials. MeV protons generate secondary electrons and, as in many lithographic processes these electrons modify the molecular structure of the resist. The energies of the proton induced secondary electrons are relatively low, and most have energies of a few tens of eVs. In the case of chain scissioning of polymethyl methacrylate (PMMA), which acts as a positive resist under proton exposure, a minimum energy of ~3.4 eV is required to break such bonds. In the case of hydrogen silsesquioxane (HSQ), 4.08 and 8.95 eV are needed to break the Si–H and Si–O bonds respectively and form a crosslinked network insoluble to developer, rendering it a negative resist. Therefore proton induced secondary electrons only modify resist material within several nano meters of the proton track and are thus ideal for resist lithography. Since protons mainly interact with the substrate electrons the path of the proton beam is very straight, resulting in smooth and well defined resist structures with practically no proximity effects, except if a "thick" resist layer is used which is comparable in thickness to the range of the proton beam in that resist material, in which case the protons will undergo increased nuclear scattering at the end of range. Calculations show that this leads to a beam spread of only a few nano meters. The exact value depends on beam energy and resist material [8]. When calculating the energy deposition due to the proton induced secondary electrons [18] it is clear that PBW has the potential to make structures below 10 nm in width in layers of at least 500 nm thickness.

In this review we will discuss achievements related to resist exposure using MeV protons. We will discuss most of the positive and negative resist materials which are used in proton exposure. We will also discuss nuclear interactions that lead to materials modification using proton beams. In this review we will only select a few materials, presenting a flavour of some of the possibilities.

2. Positive resist

2.1. PMMA

Poly(methyl methacrylate) (PMMA or Plexiglas) is a popular resist, utilized in many different lithographic processes. Primary advantages of PMMA include its simple structure, non toxic nature of the solvent (anisole), several possible dilutions allowing a wide range of resist thickness, non sensitivity to white light ($\lambda > 250$ nm), high resolution, no shelf life issues, no processing delay effects, and it can be easily removed after Ni electroplating, unless the resist has been crosslinked. With these flexible properties PMMA is a powerful resist material, which has great potential in Ni mold fabrication.

PMMA was one of the primary resists tested during the earlier study of PBW at CIBA [4]. Through these studies superior patterning capabilities (sub-100 nm) of PBW on PMMA have become well-known. Results show that trenches as small as 65 nm [19] and 50 nm narrow walls with an aspect ratio of 7 can be written in PMMA [5]. Fig. 1 shows an SEM image of parallel lines written in a 350 nm thick PMMA layer (7 aspect ratio). The structure was written with a focused 2 MeV proton beam. The photo indicates a wall width of 50 nm, reproduced with permission from [5].

CIBA has also achieved superior results for the Ni electroplating process with proton beam patterned primary PMMA molds. Ansari et al. [20] have reported a way of fabricating high-quality void-free high-aspect-ratio Ni stamps having ridges of 100 nm width and 2 μm depth. Nanoindentation and atomic force microscopy measurements of the nickel surfaces of the fabricated stamp show a hardness and side-wall roughness of 5 GPa and 7 nm, respectively. The fabricated 100 nm 3D stamps have been used to transfer test patterns into PMMA films, spin coated onto a Si substrate. PBW coupled with electroplating offers a prospective process for the fabrication of high quality metallic 3D nanostamps. Fig. 2a shows a low magnification SEM image of a Ni stamp fabricated using PBW and Ni electroplating. The stamp is a test pattern featuring two raised platforms connected by several 100 nm wide × 2 μm depth × 30 μm length high aspect ratio ridges. Fig. 2b shows an SEM image showing three of the connecting 100 nm Ni stamp ridges, and Fig. 2c shows a high magnification picture of one Ni ridge, exhibiting vertical sidewalls, and a smooth surface (7 nm rms), reproduced with permission from [20].

Uchiya et al. [21] have reported patterning of high aspect ratio structures in 5 μm thick PMMA and making use of them as a

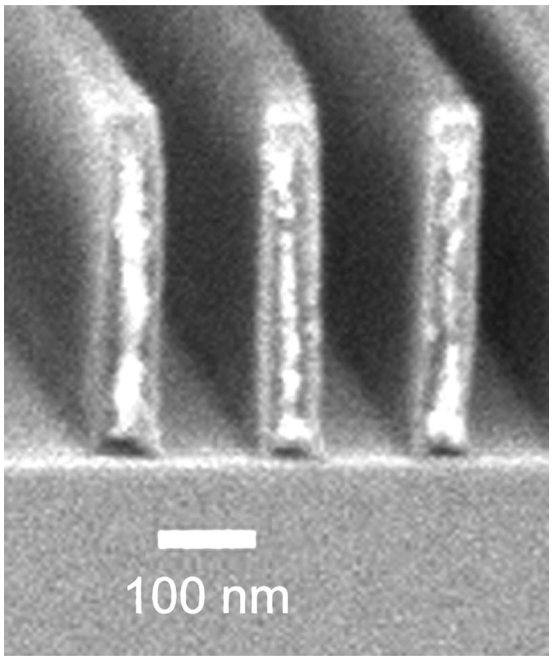

Fig. 1. SEM image of parallel lines written in a 350 nm thick PMMA layer. The structure was written with a focused 2 MeV proton beam. The photo indicates a wall width of 50 nm, reproduced with permission from [5].

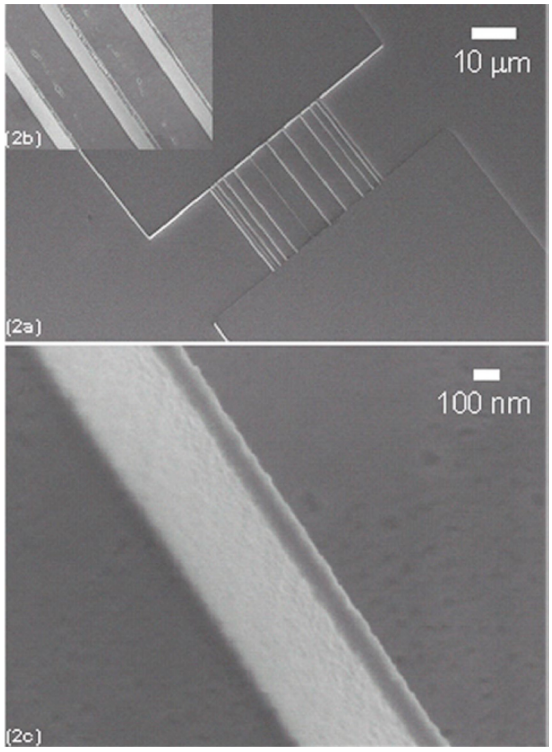

Fig. 2. (a) Low magnification SEM image of a nickel stamp fabricated using proton beam writing and nickel electroplating. The stamp is a test pattern featuring two raised platforms connected by several 100 nm wide × 2 μm depth × 30 μm length high aspect ratio ridges. (b) SEM image showing three of the connecting 100 nm Ni stamp ridges, and (c) a high magnification picture of one Ni ridge, exhibiting vertical sidewalls, and a smooth surface (7 nm rms). Reproduced with permission from [20].

replication template for Ni metallization. They used a 1.7 MeV proton beam focused down to 130 nm and they show 130 nm wide holes in the surface of the PMMA using an ion fluence of 3.8×10^{13} ions/cm^2. The Ni micro-structure, featuring 800 nm wide walls was used as a resolution standard for proton beam size measurement and the replicated Ni structures with smooth and straight side walls are useful in applications in MEMS and nano imprint lithography.

Similar Ni mold fabrication for imprint applications has been made by Tanabe et al. [22]. They used PBW on relatively thick (30 μm) PMMA layers. In order to ensure proper development of 30 μm thick PMMA high proton fluence of 3×10^{14} ions/cm^2 was used compared to the fluence of 9×10^{13} ions/cm^2 normally used for 5 μm thick PMMA. They found an improved sensitivity of 5.6×10^{13}, using isopropyl alcohol:deionized water (IPA:DI 7:3) developer combined with ultrasonic agitation, after exposure to 1.7 MeV protons in a 15 μm thick PMMA film. For Ni electroforming on patterned PMMA, Cu substrates, in place of Si, have been used to achieve void free high aspect ratio Ni structures. The oxide layer on the Cu surface is removed with EBAVATE-V37 (an acid activator for copper) to guarantee an improved adhesion of the plated Ni.

Work by Bolhuis et al. [23] deals with a comparative study of developing method and choice of developers on the performance of PBW patterned PMMA. Enhanced performance of the resist (contrast and sensitivity) was observed when GG developer (empirical mixture of water and three organic solvents, in a composition of 15 vol.% water, 60 vol.% 2-(2-butoxyethoxy)ethanol, 20 vol.% tetrahydro-1,4-oxazine (morpholine) and 5 vol.% 2-aminoethanol) was used in place of 7:3 IPA/water dip developer. In a 2.4 μm thick coated PMMA layer, contrast values of 8 and 6.1 were found and sensitivities of 7.5×10^{13} and 9.5×10^{13} ions/cm^2 for the GG developer and the 7:3 IPA/water developer respectively, followed by a DI water rinse. Typical development times of PMMA using the GG developer require about 1 min per 1 μm of film thickness, but going to nano size structures, the development time increases significantly using the GG developer, due to its high viscosity. In the above example, the 2.4 μm thick PMMA layer was developed for 40 min. Using the 7:3 IPA/water developer, the development time for nanostructures can be reduced significantly, and only 4 min is required for the 120 nm × 400 nm hole in a 2.4 μm thick PMMA layer. Employing megasonic agitation the development time can be further reduced to 1 min.

In the case of electron beam lithography (EBL) and the LIGA-process (in German: Lithography, Galvano, Abformung), it was observed that apart from the developer used, development in the presence of acoustic agitation can give rise to significant enhancement in the development rate and the performance of the resist-developer system. For EBL, the use of acoustic agitation during development has resulted in long-established minimum feature sizes below 10 nm. However, for PBW, changing the developing method from dip developing to megasonic agitation (frequency of 1 MHz) in 7:3 IPA/water did not result in any significant changes of the resist performance, except for a reduction in development time by a factor of 4 [23].

Menzel et al. [24] show, using 2.25 MeV protons, that for the exposure of PMMA (950 PMMA A15), a dose of 2.5×10^{14} up to 3×10^{14} ions/cm^2 is required to clear the irradiated areas after development. Their PMMA samples were developed for approximately 5 min in methyl isobutyl ketone (MIBK)/IPA (1:3) developer and then rinsed in ethanol and dried. Furthermore, some of the PMMA structures were hard baked on a hot plate at 100 °C for 80 s to obtain 0.5 μm details in 5 μm thick resist (10 aspect ratio). This work shows that the MIBK/IPA developer requires more fluence for complete PMMA exposure and development. Similar findings have been reported in development of electron beam

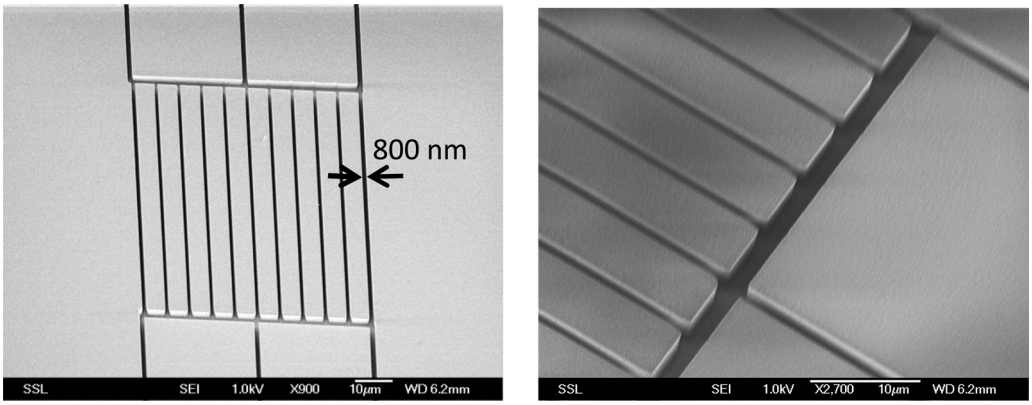

Fig. 3. SEM image of micro and nano fluidic template pattern in 8 μm thick PMGI made using 2 MeV protons with a fluence of 9.3×10^{13} ions/cm^2. Left: overview image; right: zoom in at 800 nm channels.

exposed PMMA resist [25], where the development rate of PMMA was again found to be about 1 min per 1 μm of PMMA layer thickness.

The paper by Andrea et al. [26] presents a new approach developed at the LIPSION accelerator facility for machining three dimensional structures on bulk PMMA. This method uses constant ion energy and the 3D structures are generated through the targeted irradiation of PMMA from several angles. In this way a wide range of structures such as micro screws and scaffolds for various applications can be created. This study has also considered the cross linking of PMMA due to over dosage by restricting the number of irradiation angles to three.

Direct write lithography using different incident ions namely carbon, helium and hydrogen ions on PMMA has been studied and described by Puttaraksa et al. [27]. Their investigations on the clearing chain-scissoning and cross-linking threshold fluences for 2 MeV protons, 3 MeV $^4He^{2+}$ and 6 MeV $^{12}C^{3+}$ ions in 6 μm thick PMMA on Si show that the onset fluence of cross-linking decreases with increasing electronic stopping power. For instance, 2 MeV protons with the ion stopping power of 15.2 eV/nm need fluences of 3.3×10^{13} ions/cm^2 (clearing) and 7.0×10^{14} (fully cross-linking). However, for 3 MeV $^4He^{2+}$, with an ion stopping power of 121 eV/nm requires fluences of 2.4×10^{13} ions/cm^2 (clearing) and 1.5×10^{14} ions/cm^2 (fully cross-linking).

The paper by Van Erps et al. [28] discusses the use of deep proton beam writing (DPW) using 16.5 MeV protons for fabricating micro-optical and micro-mechanical components in thicker (up to 2 mm) PMMA resist. Sakai et al. [29] have reported PBW on a 75 μm-thick acrylic film. Optimal fluence ranged from 6.0 to 9.0×10^{13} ions/cm^2 for a 3 MeV proton beam. They used 70% isopropyl alcohol (IPA) solution at room temperature for developing.

A similar fluence was found for optimal PMMA exposure for proton energies ranging from 0.5 MeV up to 16.5 MeV corrected for the difference in stopping power at the different energies, although there is a slight difference using different developers. No post exposure delay effects were reported.

2.2. PMGI

PMGI, a common lift-off resist has also been subjected to PBW [4] and the smallest feature obtained was about 1.5 μm with an aspect ratio of 8–9. In our recent studies it has been observed that smaller channels (800 nm) can easily be obtained. However, undercut is prominent, resulting in loss of structuring accuracy. Fig. 3 shows SEM images of a micro and nano fluidic template pattern in 8 μm thick PMGI made using 2 MeV protons with a fluence of about 9.3×10^{13} ions/cm^2 (left: overview image; right: zoom in at 800 nm wide channels) featuring an aspect ratio of 10. The irradiated samples were developed using GG developer. The developing rates were similar to those for PMMA, typically 1 min per 1 μm, and the developing time increased while developing narrow tranches. However, with longer developing times PMGI starts to show undercuts, a common feature in lift-off resists.

2.3. PADC

PADC (CR-39) has been shown to be a suitable material as a positive resist for PBW. 5 μm wide structures were fabricated using 2 MeV protons at fluence of 3.75×10^{14} ions/cm^2 [30]. Post-irradiation CO_2 treatment of the samples increased the radiation sensitivity of PADC, i.e. reduced the required irradiation fluence. Approximately 60% of the fluence required for untreated samples was sufficient to develop fully the CO_2 exposed structures [31].

2.4. Forturan

Foturan [32] is a photosensitive glass which has been applied to create structures by UV induced lithography or direct write laser fabrication [33]. The potential of this glass is enhanced by the fact that it can be applied in corrosive and high temperature environments, which is of major importance for applications in chemistry and biology. 2 MeV protons were used, and a fluence of only 6.3×10^{11} ions/cm^2 [34] was required for sufficient exposure. Details down to ~3 μm were achieved. Development requires more stringent safety precautions since HF is used during development.

2.5. AGAR

Larisch et al. [35] used AGAR to create patterns for biological applications. They spun 4 μm thick Agar, and exposed the film using 2.25 MeV protons at a fluence of 3×10^{14} ions/cm^2. The AGAR acts as positive resist. In the irradiated areas, the polysaccharides decompose into oligosaccharides which are soluble in water, leaving Agar-free areas for cell adhesion. They demonstrated details of dimension 15 μm and showed that the patterned area can be used to determine where EA.hy 926 cells grow.

3. Negative resist

3.1. SU-8

SU-8 is a negative tone, chemically amplified deep UV resist. In 1999, van Kan et al. achieved 1.5 μm wide SU-8 structures with aspect ratio of 24 [4]. In this work, 3D structures were also

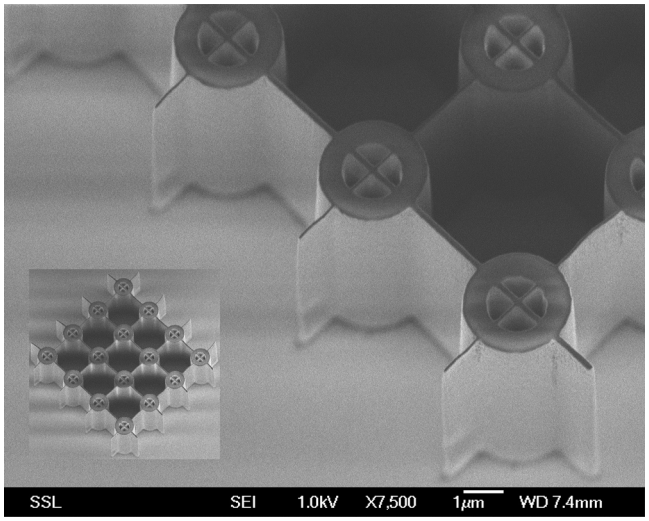

Fig. 4. High aspect ratio structure fabricated using PBW in SU-8 negative resist, showing 60 nm wall structures 10 μm deep, reproduced with permission from [36].

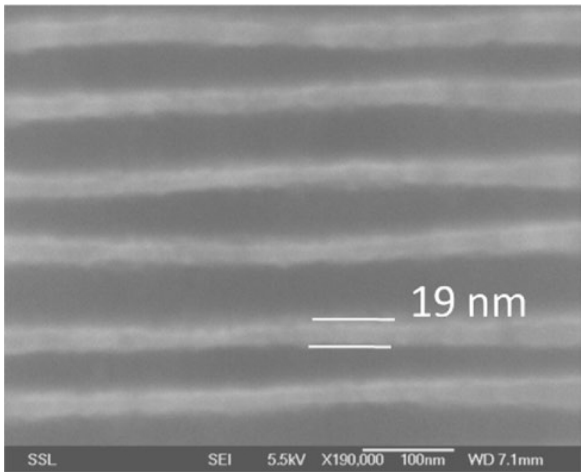

Fig. 5. SEM images of 19 nm line width with a spacing of 80 nm on 100 nm thick HSQ sample written by 2 MeV proton beam, reproduced from [19].

fabricated with different proton energies. In fact, SU-8 was the first negative resist compatible with PBW that demonstrated sub-100 nm features at CIBA in 2003 [5]. In this work, 60 nm wide lines in 10 μm thick SU-8 (aspect ratio ~ 166) were achieved using 1 MeV protons with a fluence of 1.9×10^{13} protons/cm^2. Fig. 4 shows an SEM image of high-aspect-ratio test structures fabricated using PBW in SU-8 negative resist, showing 60 nm wall structures 10 μm deep, reproduced with permission from [36]. No post exposure bake was required. In fact, applying a post exposure bake compromised the minimum feature size obtained. However to ensure enough rigidity, a post exposure bake at 100 °C for 2 min was found necessary, following UV patterning of SU-8 resist. This guarantees long mold life in PDMS casting applications, allowing more than 200 replications [37].

In 2009, Furuta et al. developed 3D-electric micro filters equipped with a high-aspect-ratio pillar array with a height of ~15 μm and a diameter of ~1 μm [38]. The pillar array was fabricated using a 15 μm thick SU-8 resist layer on silica substrate, patterned by 1.7 MeV protons at dose of 6.3×10^{13} ions/cm^2. The relatively high fluence was chosen in order to ensure that the pillars remained standing. Menzel et al. used 2.25 MeV PBW to create grayscale structures in SU-8 at doses of $1.8–30.6 \times 10^{12}$ ions/cm^2 [39]. This resulted in structures with a recognizable gradient height profile which, however, exhibits instabilities and no sharp structure edges in the grayscale area.

3.2. HSQ

HSQ is another high resolution negative resist for PBW. In 2010, van Delft et al. fabricated 20 nm wide structures in a 20 nm thick HSQ using 10 keV H^{3+} at fluence of 7.5×10^{13} ions/cm^2 [40]. 22 nm [6] and 19 nm [19] wide structures were achieved in 850 nm and 100 nm thick HSQ respectively using 1 MeV protons. Fig. 5 shows an SEM image of 19 nm line width with a spacing of 80 nm on 100 nm thick HSQ sample written by 2 MeV proton beam, reproduced from Microsystem Technologies [19].

HSQ is developed in a 2.38% tetramethyl ammonium hydroxide (TMAH) solution for 1–2 min, followed by a DI water rinse. Even for features down to 19 nm in size, this is sufficient. The sensitivity varies significantly from batch to batch ($1.9–13 \times 10^{13}$ ions/cm^2), and at the same time the contrast also varies drastically from 1.2 up to 10. In the latter case a large fluence is required. These variations in processing conditions plus the rather short self-life require the user to calibrate HSQ for every batch, and from time to time, to guarantee reproducible results at the nm level. Once the resist is calibrated, the HSQ performs very reliably and the exact structure size depends only on the beam size and fluence used.

Despite the high resolution reported in SU-8 and HSQ, they have limited applications in PBW. One main drawback for SU-8 is the fact that it cannot be removed after Ni electroplating. And HSQ has a limited height of less than 1 μm. Therefore alternative negative resists are being investigated with various levels of success.

3.3. ma-N

ma-N series resist (Micro Resist Technology GmbH) has several formulations with different characteristics. ma-N 440 and ma-N 490 were irradiated using $0.7 \times 10^{13}–1.2 \times 10^{14}$ ions/cm^2 using 2.25 MeV H^+ to investigate the dependence between fluence of protons and depth of resist [39]. A micro-Fresnel-lens 150 μm in diameter and 12 μm high was created by PBW. At fluence of 3.7×10^{13} ions/cm^2, structures down to 25 μm can be achieved in 7–28 μm thick ma-N. These resists are suitable for grey scale lithography but the obtained structures are rather porous, limiting some of the applications.

ma-N 2401 and ma-N 2410 are both negative tone photoresists which belong to the ma-N 2400 series. ma-N 2401 is a high resolution EBL and deep UV resist. 60 nm wide lines in a 100 nm thick film have been achieved using 1 MeV protons at fluence of 2.5×10^{13} ions/cm^2 [41]. ma-N 2410 is capable of fabricating structures down to 250 nm lines in 600 nm thick film using 1 MeV protons at fluence of 4.38×10^{13} ions/cm^2 [42]. Fig. 6a shows a 60 nm wide line in 100 nm thick ma-N 2401 via 1 MeV proton beam writing Fig. 6b shows a 100 nm wide line in 100 nm thick ma-N 2401 (30° tilt), reproduced with permission from [41]. Ni plating is limited to 500 nm wide and 1 μm high structures due to the difficulties in removing the resist after Ni plating.

3.4. AR-P 3250

The AR-P 3200 series photoresists from ALLRESIST [43] are positive tone resists that undergo chain scission via UV exposure (365 nm). When AR-P 3250 was subjected to PBW [44], it was observed that, for a proton fluence of about 2×10^{13} ions/cm^2 and above, the resist cross links like a negative resist. A sequential UV-exposure is required to render the resist surrounding the PBW fabricated structures developable. Even at a lower proton fluence of 6×10^{11} ions/cm^2 cross linking was observed, although it is

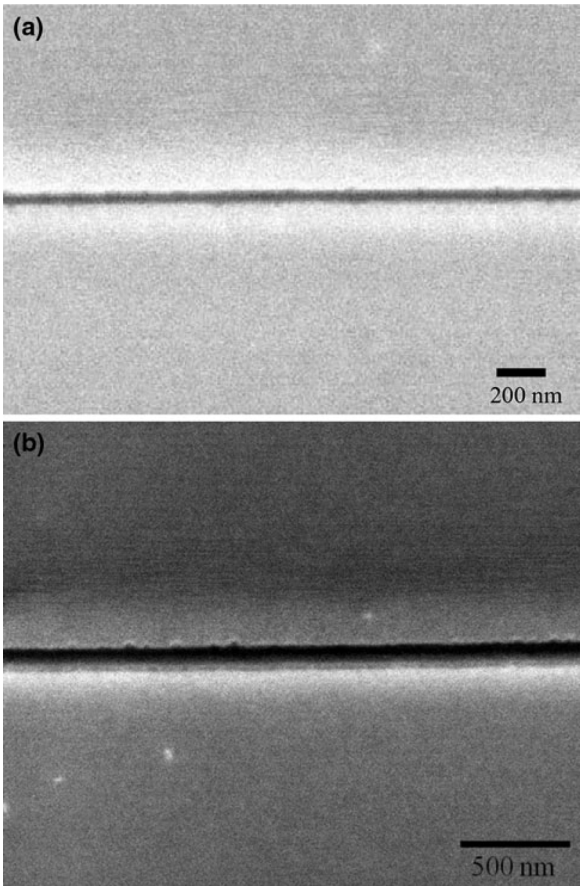

Fig. 6. (a) A 60 nm wide line in 100 nm thick ma-N 2401 via 1 MeV proton beam writing; (b) 100 nm wide line in 100 nm thick ma-N 2401 (30° tilt), reproduced with permission from [41].

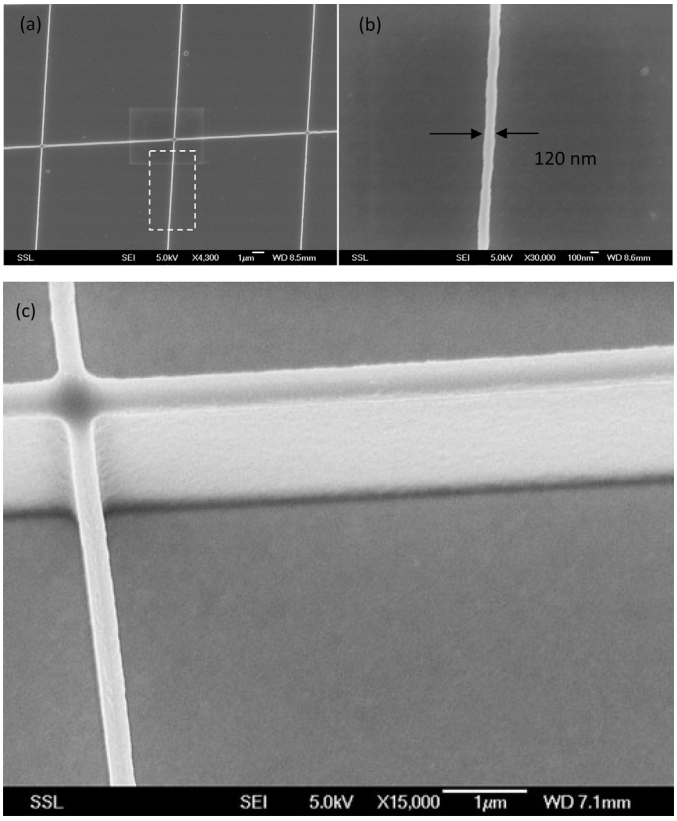

Fig. 7. (a) Electron microscope image of grids in a 280 nm thick layer featuring 120 nm wide lines. (b) A high magnification SEM image of the 120 nm wide line in 280 nm thick AR-P 3250:AR300-12 = 1:3 diluted before spincoating. (c) 330 nm wide line written in 3.5 μm thick AR-P 3250 via 1 MeV proton beam writing, 6 min UV exposure and 60 s development, reproduced with permission from [41].

incomplete. This behavior of AR-P 3250 resist (cross linking with protons and chain scissioning with UV) is a useful finding. With this resist 3–11 μm layer thickness can be easily patterned. 330 nm wide structures in a 3.5 μm thick film were achieved using 1 MeV protons at a fluence of 3.1×10^{13} ions/cm^2 [41]. In fact, even smaller structures can be realized, however, the structures all fell down because of the high aspect ratio.

It was also observed that the cross linking by proton beam is affected to some extent during the sequential flood UV exposure process, especially for smaller features. In order to ensure the fidelity of the cross linked high aspect ratio structures in AR-P 3250, higher proton fluences and well controlled UV exposure should be employed [41]. Thinner layers of AR-P 3250 were obtained by mixing AR-P 3250 and AR 300-12 (thinner from AllResist GmbH) in the ratio of 1:3. The mixture, when spincoated at 4000 rpm for 30 s followed by a pre bake at 95 °C for 30 s yields a layer thickness of 280 nm. Structures down to 120 nm were fabricated using 1 MeV protons at fluence of 3.1×10^{13} ions/cm^2 [41].

AR-P 3250 and AR-P 3250 mixed with AR 300-12 behave similarly under proton irradiation followed by UV exposure. Micro and nanostructures produced in this way are particularly useful in replicating features in nickel through the electroplating process. The conventionally used high aspect ratio SU-8 resist presents difficulties during resist removal from the molded Ni. However AR-P 3250 and AR-P 3250 mixed with AR 300-12, were found to be easily and completely removable from the Ni molds, which were subsequently used as metallic stamps for nano imprinting and injection molding applications [41]. Fig. 7a shows an electron microscope image of grids in a 280 nm thick layer featuring 120 nm wide lines. Fig. 7b shows a high magnification SEM image of the 120 nm wide line in 280 nm thick AR-P 3250, diluted in AR300-12 (1:3, v/v) before spincoating. Fig. 6c shows 330 nm wide line written in 3.5 μm thick AR-P 3250 via 1 MeV proton beam writing, 6 min UV exposure and 60 s development, reproduced with permission from [41].

Fig. 8 shows a contrast curve for a 5 μm thick spin coated AR-P 3250 layer as a function of fluence using 1 MeV protons and an optimized flood UV exposure. Here 500 μm × 500 μm structures were written with the proton beam. A fitted contrast value of 1.6 ± 1.0 is obtained from these measurements. Calculation of PBW contrast values as a function of feature size and shape have been performed

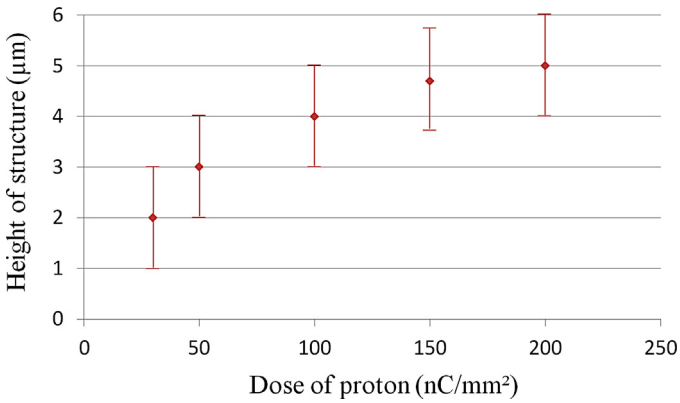

Fig. 8. AR-P 3250 contrast curve, after development following exposure to a 1 MeV proton beam and 10 min UV exposure. The size of the structures is 500 μm × 500 μm.

Table 1
Contrast values obtained for 5 μm thick AR-P 3250 as a function of PBW feature size and shape.

Feature size	Contrast
500 nm lines [41]	3.5 ± 0.5
10 μm × 10 μm [44]	2.0 ± 0.5
500 μm × 500 μm	1.6 ± 1.0

In CIBA AR-P 3210 has been tested in combination with PBW up to 40 μm in thickness. Proton fluences as high as 1.8×10^{14} were used followed, by UV flood exposure. However, no cross linking was observed, as is the case with AR-P 3250.

for AR-P 3250, where it was found that the contrast improves with decreasing feature sizes. In Table 1, the results are summarized.

3.5. ma-P

ma-P is a UV positive resist (Micro Resist Technology GmbH), which shows cross-linking through PBW similar to AR-P 3250. ma-P 1275 has been tested for UV exposure and proton beam writing, achieving features with smooth and straight sidewalls [45]. The optimum fluence for PBW experiments in combination with UV lithography for this resist is around 3.1×10^{13} ions/cm^2. Ni molds formed on these resist molds are completely free of resist and are identical in smoothness and size to the original polymer structures. However, high aspect ratio patterning and resist removal after electroplating presented difficulties due to post exposure delay effects and a narrow window for PBW fluence. If the fluence is too high, the resist cannot be removed from the Ni mold. This particular resist may be useful for applications where larger low aspect ratio structures with smooth and straight sidewalls are required.

3.6. TADEP

TADEP is a negative tone chemically amplified photoresist. In 2008 Chatzichristidi et al. reported using 2 MeV protons at a fluence of 1.9×10^{14} ions/cm^2 to fabricate structures down to 1.5 μm in 11 μm thick film [46]. Even smaller structures down to 110 nm in 2 μm thick film were achieved at CIBA-NUS using 2 MeV protons [47]. Fig. 9 (left) shows an SEM image of 280 nm wide lines written with 2 MeV protons in a 12 μm thick layer of TADEP, featuring an aspect ratio of 42. In Fig. 9 (right), a 1.5 μm thick layer of TADEP was structured with a 2 MeV proton beam to yield 110 nm wide lines (13.6 aspect ratio). Both exposures were performed with a fluence of 1.6×10^{13} ions/cm^2. It must be noted that exposure and development conditions have not been optimized for this resist. Also the removal of this resist is not convincing and needs to be optimized.

3.7. KMPR

KMPR resist has chemical and process properties similar to those of SU-8. A sensitivity of 6.2×10^{12} ions/cm^2 and a contrast of 2–3 were observed for 2 MeV protons cross-linking this negative resist (7.6 μm thick). Development using 2.38% TMAH for 5 min [48] is sufficient. It was found that KMPR could not be reproducibly removed after Ni electroplating. A contrast around 2.2 was found if no post exposure was applied, but when a post exposure bake without any development delay was applied, the contrast was around 3.3. Structures with details down to 1 μm can be achieved with good fidelity at a fluence of 8.8×10^{13} ions/cm^2 in a layer of 7.6 μm thickness. By lowering the fluence to 2.8×10^{13} ions/cm^2, and developing without post-exposure bake after a one week delay, a 750 nm wide line was obtained featuring an aspect ratio of 10. We note, however, that the KMPR then loses rigidity.

3.8. EPO core

EPO core is also a negative tone photoresist, where a 42 μm thick film can be developed in mr-Dev 600 (Micro Resist Technology GmbH) (3 min) followed by a DI water rinse. In the case of EPO core, a sensitivity of 6.25×10^{11} ions/cm^2 and a contrast of 0.9 ± 0.3 were observed for 2 MeV protons [48]. Structures down to 10 μm in 40 μm thick film can be achieved.

3.9. WL-7154

WL-7154 is a UV-sensitive negative resist and shows high sensitivity for PBW (2.5×10^{12} ions/cm^2). A contrast of 6 ± 1 was found using 2 MeV protons [49]. Using 1 MeV protons at a dose of 5.0×10^{12} ions/cm^2, 260 nm wide walls were achieved in a 1.4 μm thick film, where the higher fluence was required to guarantee enough cross linking to support the nanowalls [42]. WL-7154 shows promise for high aspect ratio nano fabrication but due to its high sensitivity, any scattered beam will give rise to a thin residual layer of resist on the Si substrate. Therefore proton structuring and development of WL-7154 requires more fine tuning before it can be effectively used in PBW applications.

3.10. TiO_2

Titanium dioxide has shown the potential for application in solar cells [50], optical waveguides [51], gas sensors [52] and electrochromic displays [53]. Patterning TiO_2 is challenging especially in miniaturizing devices. For thin layer applications a TiO_2 based resist has been developed by Saifullah et al. [54]. They have shown details down to 10 nm in electron beam lithography. Thick films can be easily patterned using PBW [49]. A sensitivity of 5×10^{15} ions/cm^2 has been found and a contrast of 2.3 ± 0.5 using 1 MeV proton irradiation. One major drawback is the crack formation in 7 μm thick spincoated films. More research and brighter ion sources are required to optimize TiO_2 as a successful resist in PBW.

3.11. PDMS

Saito et al. [55] have used PDMS in PBW experiments. They employed a 1 MeV proton beam to irradiate 13 μm thick spincoated layers of PDMS. During spin-coating, only the base agent (Sylgard 184) was coated for 60 s at 8000 RPM to yield a 13 μm thick layer. The PDMS acts as a negative resist under proton irradiation. In the PBW process, no curing is needed, either before or after development, since the PDMS prepolymer becomes crosslinked via proton irradiation [56]. The PDMS films were developed with a solution of THF–CH_3CN (8:2) for 2 min at 60 °C. Saito et al. [55] also investigated the sensitivity of PDMS as a function of substrate material. Their conclusion was that the required fluence can be as low 1.3×10^{12} ions/cm^2 if the substrate is sufficiently conductive. This can be assured by coating a thin layer of Au (13.5 nm) on a Si wafer before applying PDMS. On the other hand, if the PDMS is coated directly on the Si wafer the required fluence increases to 3.1×10^{12} ions/cm^2 and if the PDMS is applied on silica glass the required fluence shoots up to 4×10^{14} ions/cm^2. The best contrast (2.0) is observed on Au coated Si wafers. They proceeded to use the grey scale effect of PDMS under proton irradiation to produce spherical structures which act as micro lenses, whose typical diameter is 40 μm and typical height is 13 μm.

3.12. Diaplate

DiaPlate 133, is a negative tone thick photoresist, developed by CSEM [57] based on acrylic chemistry. It can be processed at thicknesses up to 700 μm and was designed to replace SU-8. It is

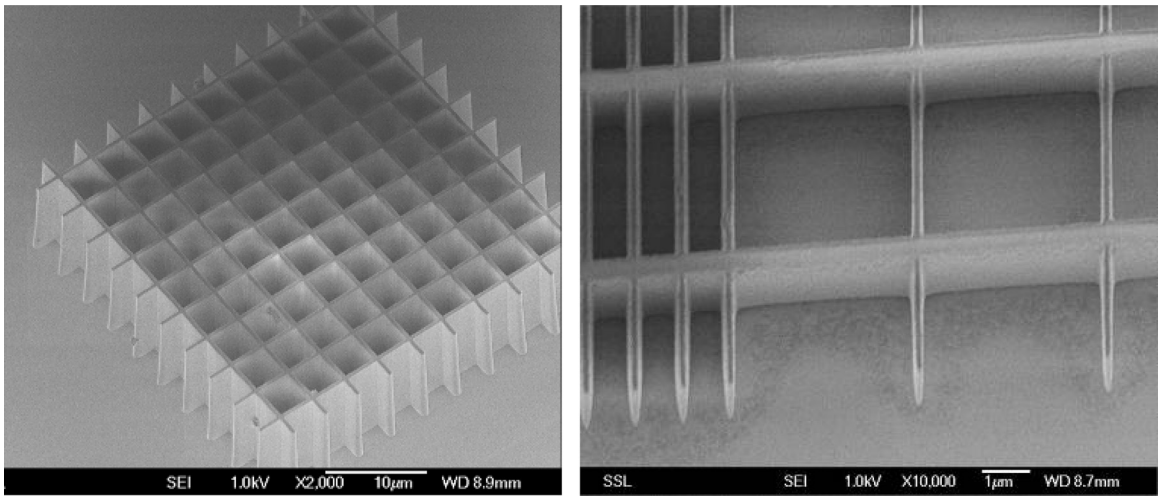

Fig. 9. (Left) SEM nano lines written in 12 μm thick TADEP, featuring 280 nm wide lines. (Right) A 1.5 μm thick layer of TADEP featuring 110 nm wide lines. Both exposures were performed with 2 MeV protons (1.6×10^{13} ions/cm^2).

especially sensitive to UV in the range of 300–450 nm and its main solvent is propylene glycol monomethyl ether. It has the advantages of aqueous processing, good mechanical flexibility, and ease of stripping. Gonin et al. [58] have used a 2.7 MeV proton beam to write squares of 70 μm × 70 μm in diaplate (70 μm thick). After proton exposure the resin requires a post-exposure bake of 5 min at 80 °C followed by a spray development at 2 bars with an aqueous solution of 1% Na_2CO_3 at 30 °C for 6 min. Sodium carbonate (Na_2CO_3) is a very common product used to develop printed circuit boards and is therefore very easy to handle and manage. Finally the substrate is rinsed with DI water. The optimal fluence was 6.3×10^{12} ions/cm^2, but lower fluences were not reported.

4. Materials modification

Here we will discuss nuclear interactions that lead to materials modification using proton beams. In this section we will only select a few materials, presenting a flavour of some of the possibilities.

4.1. Si

At CIBA, Teo et al. have reported fabrication of three dimensional multilevel cross structures and freestanding Si structures, using high energy proton or helium ion beams [59], followed by electrochemical etching for micro-fabrication in bulk p-type silicon. The ion-induced damage increases the resistivity of the irradiated regions and slows down the formation of porous silicon. A raised structure of the scanned area is left behind after removal of the unirradiated regions with potassium hydroxide. The thickness of the removed material depends on the irradiated dose at each region so that multiple-level structures can be produced with a single irradiation step. A free standing uniform array of closely packed, high aspect-ratio Si pillars was obtained by single spot irradiations by a focused proton beam. Each spot had an accumulated fluence of 5×10^{16} protons/cm^2. The sample was then etched for 15 min with a current density of 40 mA/cm^2. The resulting pillars were 4.5 μm high with a diameter of 0.6 μm, and a periodicity of 2 μm. By irradiation under similar conditions but aligning the incident ion beam with an axis or set of crystal planes of Si, the ion beam can be channeled, which reduces the probability of nuclear collisions with silicon atoms. This results in a significant reduction of the damage caused by the ion beam close to the surface. Reduction of damage near the surface regions results in fabrication of much sharper and thinner pillars, with a radius of curvature of about 15 nm at the tip, sloped steeply at an angle of 85°. Fig. 10 shows an SEM image of sharp Si spikes obtained when the beam was channeled along the [1 0 0] crystal axis. The inset shows a close-up SEM image of the tip, reproduced with permission from [59].

For multilevel structures protons of different energies (0.5 MeV and 2 MeV) were used to make elevated and supporting structures respectively. Apart from fabricating a multilevel structure by multiple dose exposures in a single irradiation, PBW has also been used to produce patterned porous Si for a range of different applications [60]. Porous Si is of interest because of its tunable photoluminescence (PL) and electroluminescence (EL) properties, which enable production of light-emitting devices with microelectronics compatibility. Tuning of the PL intensity and wavelength has been obtained by controlling the local resistivity as a function of fluence. PBW studies on porous Si have shown that there are two resistivity regimes of p-type Si where PL is affected in different ways by ion irradiation: of low-resistivity (~0.01 Ω cm)

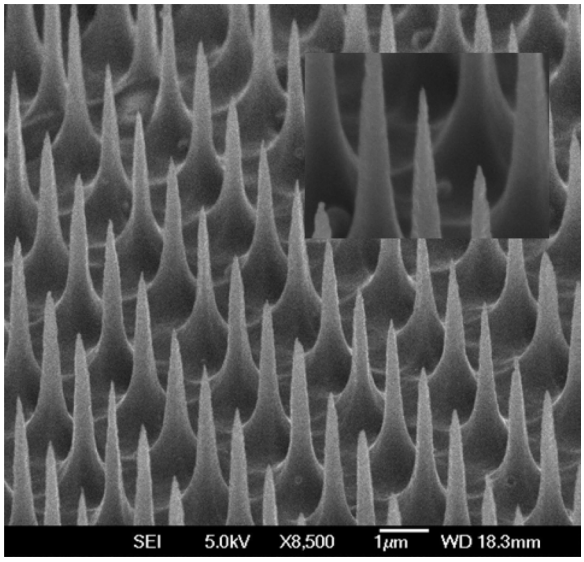

Fig. 10. Sharp Si spikes obtained when the beam is channeled along the [1 0 0] crystal axis. Close-up SEM of the tip is shown in the inset picture, reproduced with permission from [59].

wafers (where irradiation primarily results in a large PL increase), whereas for moderate resistivity (0.1–10 Ω cm) wafers, irradiation primarily results in a large PL wavelength red shift.

Recent work on Si modification by Azimi et al. [61] demonstrates the fabrication of complex curved three-dimensional Si microstructures. The ability of high energy protons to create localized defects at the end of range is used to machine complex 3D Si structures within the bulk Si after subsequent anodization and removing the porous silicon.

Liao at al. [62] have studied proton induced high resistivity trap levels in n and p type Si. It was observed that under the intended conditions of low-current proton beam at 15 and 30 MeV effective single trap level E_T was found to be about +0.24 eV in n-Si and −0.34 eV in p-Si, measured from the center of the energy bandgap. The revealed deep levels in the bandgap were consistent with the evidence of severe charge carrier removal caused by the proton treatments.

Kim et al. [63] have reported the use of a 3 keV low-energy proton beam to irradiate a silicon substrate for selective modification of the surface, using a typical fluence 1×10^{16} ions/cm^2. The proton beam-irradiated silicon substrate was covered with a silicon oxide layer of about 6–7 nm due to the incorporation of oxygen after exposure to ambient air. The silicon oxide layer produced by the proton beam is highly resistant to HF treatment which is typically used to remove silicon oxide on a substrate. After HF etching this proton irradiated Si was used to selectively grow carbon nanotubes (CNTs) after adsorption of Fe–Mo particles on the irradiated areas.

4.2. GaAs

Apart from Si modification, study of technologically important materials such as solar cell materials and conducting oxides under accelerated simulating processes with protons are useful to understand their behavior under ambient proton flux. In case of GaAs based solar cells for space applications, low-energy proton irradiation is one of the important factors which affect the performance. The proton flux encountered in orbit is much lower than that used during ground-based radiation experiments, called accelerated simulating process. Hu et al. [64] showed that under low-energy proton irradiation, GaAs solar cells generally degrade due to displacement damage effects. Furthermore, the degradation in electrical properties can be enhanced by increasing the proton energy and fluence. The proton energies were selected as 40, 70, 100 and 170 keV. The proton fluences were in the range of 2×10^{10}–1×10^{13} ions/cm^2. The proton fluences that cause surface degradation are lower than typical fluences used for micro-machining of GaAs through nuclear damage. Studies of (1 0 0) p-type GaAs irradiated with 2.28 MeV protons and fluences in the range from 1.25×10^{14} ions/cm^2 to 1×10^{18} ions/cm^2 showed a linear dependence of structure height on ion fluence [65].

In p-type GaAs, pillars with diameters of 1.3 μm and structures with an aspect ratio of 12.5 were achieved using 2.25 MeV protons [65]. In this study (1 0 0) p-type GaAs was irradiated with 2.25 MeV protons at fluences in the range from 3.8×10^{14} ions/cm^2 to 1.0×10^{18} ions/cm^2, at the ion beam laboratory LIPSION, and subsequently electrochemically etched with 10% KOH. A linear dependence of structure height on ion fluence was established. In this way, pyramid-like structures as well as concave-shaped structures could be created. GaAs showed a lateral anisotropic etch behavior during the development step with preferential etching along the [0 1 1] directions. The surface roughness and the change of conductivity were investigated by atomic force and scanning capacitance microscopy, respectively [66].

4.3. Kapton

Kim et al. [67] have reported the effect of MeV protons on mechanical behavior such as tensile strength and elongation of ITO/aluminum-coated Kapton that is known to be one of the most useful polymers for space missions. The mechanical properties (tensile strength and elongation) of specimens irradiated with high-energy protons were lower than those of samples after irradiation with low energy protons. A considerable improvement in the mechanical properties was observed due to proton irradiation at lower fluences. This was attributed to the unique characteristics of the molecular structure of Kapton. The tensile strength and elongation properties improved after an equivalent total exposure of 3 years in orbit and at a fluence of approximately 9.5×10^{13} ions/cm^2, using 10 and 30 MeV protons.

4.4. TiO_2

Work by Vujisic et al. [68] reports on the effects of proton radiation on titanium dioxide used in memristors. It was found that exposure of a titanium dioxide memristor to ion beams can influence the device's operation in several ways. Through simulation studies, they have shown that generation of oxygen ion/oxygen vacancy pairs in the oxide is expected. Appearance of oxygen vacancies in the stoichiometric TiO_2 layer can cause its resistance to drop, causing changes in the memristor electrical behavior.

4.5. PTFE

Kitamura et al. [69], presented an approach to pattern Polytetrafluoroethylene (PTFE, $-(CF_2-CF_2)_n-$) and fluorinated ethylene propylene (FEP, $-(CF_2-CF_2)_n-(CF_2-CF(CF_3))_m-$) also known as Teflon using combined focused 3 MeV proton and broad beam 250 keV N_2^+ irradiation. They first irradiated a 100 μm FEP sheet Neoflon (Daikin Industries Ltd.) with 3 MeV protons using fluences between 2.5×10^{11} and 2.5×10^{13} ions/cm^2, followed by a 250 keV N_2^+ exposure (2.0×10^{15} ions/cm^2). This resulted in spikey topography which can potentially be used in bio applications. Proton exposure alone above 1×10^{12} ions/cm^2 leads to bubble formation.

Kitamura et al. [70] exposed 500 μm thick PTFE sheets (Nichias Corp) with 3 MeV protons with fluences ranging from 1.2×10^{12} to 6.2×10^{13} ions/cm^2. There is no development required but the shape created depends on the writing path strategy. Pillars can be created up to 250 μm tall whereas a 3 MeV proton beam has a limited range of only 88 μm in PTFE. They have a size of 10 μm at the top and 50 μm at the base using a fluence of 3.1×10^{13} ions/cm^2. The beam path is spiralling out to generate the right pressure in the material to create these porous pillars which might find applications in the medical field.

4.6. PDMS

Szilasi et al. [71] used PDMS where the base polymer and the curing agent were mixed with the volume ratio 10:1 to fabricate structures through swelling. The mixture was poured in a Petridish to cast a 3 mm thick layer and was cured for 36 h at 25 °C. Next a 2 MeV proton irradiation caused significant swelling perpendicular to the surface, resulting in 8 μm wide and 20 μm tall PDMS structures. It was observed that there is a compaction at the original surface, and a swelling at the edge of the irradiated area. The rate of compaction did not depend strongly on the delivered fluence (2.5×10^{14}–1.0×10^{15}/cm^2). Huszank et al. observed similar structure sizes but reduced the PDMS curing to 30 min at a temperature of 125 °C using 2 MeV protons at a fluence of 3.1×10^{14} ions/cm^2 [72].

Table 2
Resist characteristics for PBW.

Resist	Type neg./pos	Fluence (ions/cm^2)	Proton energy (MeV)	Smallest feature Written	Aspect ratio in resist	Smallest feature in Ni	Contrast
PMMA [5,19]	P	$5.0–9.4 \times 10^{13}$	2	20–30 nm[a]	100	65 nm	8
SU-8 [5]	N	1.9×10^{13}	1	60 nm[a]	166	[b]	[c]
HSQ	N	$1.9–13 \times 10^{13}$	2	19 nm [19][a]	40 [6]	[e]	1.2–10
PMGI	P	9.3×10^{13}	2	800 nm	10	[c]	[c]
WL-7154 [42]	N	$2.5–5.0 \times 10^{12}$	1	260 nm	5	[c]	6
TiO2 [49]	N	5.0×10^{15}	2	5 μm	1.4	[c]	2.3
Si [59]	N	5.0×10^{16}	2	15 nm tip implanted in channeling geometry	15 nm at the tip 600 nm at the bottom, sloped steeply at an angle of 85°	[c]	[c]
TADEP [47]	N	$1.6–15 \times 10^{13}$	2	110 nm	18	[e]	[c]
ma-N 2401 [41]	N	2.5×10^{13}	1	60 nm[a]	1.6	[b]	[c]
ma-N 2410 [42]	N	$4.4–13 \times 10^{13}$	1	250 nm	2.4	500 nm[d]	[c]
ma-N 440 ma-N 490 [39,78]	N	$0.7–12 \times 10^{13}$	2.25	400 nm	[c]	2 μm	[f]
AR-P 3250 [41]	N	$1.9–3.1 \times 10^{13}$	1	330 nm	10.6	330 nm	1.6–3.5
AR-P 3250:AR 300-12 (1:3) [41]	N	3.1×10^{13}	1	120 nm	2.3	120 nm	
KMPR [48]	N	8.8×10^{13}	2	750 nm	10	[b]	2.1–3.3
EPO core [48]	N	6.25×10^{11}	2	10 μm	4	[c]	0.9
ma-P 1275 HV [79]	N	1.3×10^{13}	1	10 μm	0.17	10 μm[d]	[c]
Diaplate [58]	N	6.3×10^{12}	2.7	10 μm	7	[c]	[c]
PADC (CR-39) [30]	P	$22–38 \times 10^{13}$	2	5 μm	0.0048	[c]	[c]
Forturan [34]	P	6.3×10^{11}	2	3 μm	13.3	[c]	[c]
GaAs [80]	N	6.3×10^{16}	2	12 μm	1.4	[c]	[c]
AGAR [35]	P	3.0×10^{14}	2.25	15 μm	0.3	[c]	[c]
PDMS [55]	N	$0.13–40 \times 10^{13}$	1	10 μm	1.3	[c]	2.0

[a] Limited by beam focus.
[b] Cannot be removed.
[c] No data.
[d] Limited by resist removal.
[e] Data not convincing.
[f] Values could be calculated from the results obtained by Menzel et al. [39].

4.7. CR-39

CR-39 is a thermoset polymer (allyl-diglycol-carbonate, $C_{12}H_{18}O_7$, q 1/4 1:31 g/cm^3), and it is widely used in applied nuclear physics as the basic material for Solid State Nuclear Track Detectors (SSNTD). 2 MeV protons were used, by Rajta et al. [30], here a fluence of $1–3 \times 10^{14}$ ions/cm^2 was required for sufficient exposure. A proton exposure in CR-39 causes a change in the optical diffraction of the material which can be used in microphotonics applications, where details down to 10 μm have been resolved.

5. Discussion and conclusion

Abesselam et al. [73] investigated stoichiometric changes due to 1.1 MeV proton irradiations of polyethylene terephthalate (PET) thin films, using ion fluences in the range 5×10^{13} to 4×10^{15} ions/cm^2. They found that at the lowest fluence (5×10^{13}) there is no noticeable material loss, whereas at 5×10^{14} ions/cm^2 there is an onset of material degradation.

As a summary many of the known resist materials for PBW are listed in Table 2, showing the smallest feature written, highest aspect ratio achieved, and Ni plating performance as well as contrast values for each of the different resist materials.

Summarizing operation parameters for PMMA we saw that the irradiation window for patterning with ions is the largest when using protons. There is a factor of 21 between the clearing fluence of 3.3×10^{13} ions/cm^2 and fully cross-linking at 7.0×10^{14} ions/cm^2, and this window narrows going to heavier ions. Comparing the different developers for PMMA, the highest sensitivity is achieved with the GG developer (3×10^{13} ions/cm^2), the IPA:DI (7:3) developer requires a 30–90% higher fluence ($7–9 \times 10^{13}$ ions/cm^2), whereas the MIBK/IPA developer seems the least sensitive ($2.5–3 \times 10^{14}$ ions/cm^2) for 2 MeV protons. Since the GG developer is rather viscous, coupled to the fact that PMMA behaves as negative resist at a fluence of 7×10^{14} ions/cm^2, the IPA:DI (7:3) developer is the most suitable developer for PBW experiments.

Using He^+ beams at low energies (30 keV) Winston et al. and Sidorkin et al. [74,75] have shown details down to 5–10 nm in thin (~10 nm) HSQ resist layers. Minimum feature sizes observed with PBW in HSQ resist are walls of 19 nm wide in 100 nm thick HSQ, closely matching the proton beam size. These results with He^+ and proton beams suggest that HSQ can be patterned with proton beams down to sub 10 nm dimensions, featuring high aspect ratios. To realize this, brighter proton sources are needed.

Using similar beam sizes in PMMA and HSQ the observed structures are significantly larger in PMMA [19], there is no clear explanation for this phenomenon at the moment and more research is required to find a suitable explanation.

If a negative resist is needed to fabricate high aspect ratio structures in Ni, AR-P 3250 has recently been shown to be a powerful candidate. Operating parameters for AR-P 3250 are relatively narrow and fine tuning of the required proton dose, UV exposure dose and development time is required to achieve smooth Ni structures free from resist residues.

Besides Ni molds for nano imprint lithographic experiments, PBW fabricated resist molds can be a good alternative allowing for fast replication of nanofluidic lab-on-chip devices for single DNA

molecule studies with nanofluidic channels having a cross section down to 100 nm × 60 nm [37]. These lab-on-chip devices have also been used for manipulating single DNA molecules in nano confinement [76] as well as for large scale genome mapping with a resolution of 1.5k base pair [77].

In an accurately calibrated PBW system, resists like PMMA, HSQ and SU-8 perform reproducibly i.e. for a given beam size, fluence and beam energy, the same structure size is obtained. No post exposure delay effects have been observed for these resists. For AR-P and ma-P processing, conditions are more delicate and post exposure delay effects also play a role.

Relatively limited contrast data are available but the current data suggest that there is a positive correlation between high contrast values and sub 100 nm structuring capabilities of resist like PMMA and HSQ.

Several effective resist materials have been reviewed. However, more research is needed into resist materials to fully utilize the potential of PBW.

Acknowledgment

We acknowledge the financial support from the MOE Singapore (R-144-000-312-112).

References

[1] R.L. Seliger, R.L. Kubena, R.D. Olney, J.W. Ward, V. Wang, J. Vac. Sci. Technol. 16 (1979) 1610.
[2] Ilesanmi Adesida, Nucl. Instrum. Methods B7/8 (1985) 923–928.
[3] K.H. Brenner, M. Frank, M. Kufner, S. Kufner, Appl. Opt. V29 (1990) 3721.
[4] J.A. van Kan, J.L. Sanchez, B. Xu, T. Osipowicz, F. Watt, Nucl. Instrum. Methods B158 (1999) 179.
[5] J.A. van Kan, A.A. Bettiol, F. Watt, Appl. Phys. Lett. 83 (2003) 1629, http://dx.doi.org/10.1063/1.1604468, AIP Publishing LLC.
[6] J.A. van Kan, A.A. Bettiol, F. Watt, Nano Lett. 6 (2006) 579.
[7] J.A. van Kan, P. Malar, A. Baysic de Vera, Rev. Sci. Instrum. 83 (2012), 02B902-1–02B902-3.
[8] J.A. van Kan, T.C. Sum, T. Osipowicz, F. Watt, Nucl. Instrum. Methods B161 (2000) 366.
[9] C.N.B. Udalagama, A.A. Bettiol, F. Watt, Nucl. Instrum. Methods B260 (2007) 384.
[10] A.A. Bettiol, J.A. van Kan, T.C. Sum, F. Watt, Nucl. Instrum. Methods B181 (2001) 49.
[11] A.A. Bettiol, C.N.B. Udalagama, J.A. van Kan, F. Watt, Nucl. Instrum. Methods B231 (2005) 400.
[12] P. Tuteleers, P. Vynck, H. Ottevaere, V. Baukens, G. Verschaffelt, S. Kufner, M. Kufner, A. Hermanne, I. Veretennicoff, H. Thienpont, SPIE 3490 (1998) 409.
[13] C. Debaes, J. Van Erps, M. Vervaeke, B. Volckaerts, H. Ottevaere, V. Gomez, P. Vynck, L. Desmet, R. Krajewski, Y. Ishii, A. Hermanne, H. Thienpont, New J. Phys. 8 (2006) 270.
[14] D. Mangaiyarkarasi, Ow Yueh Sheng, M.B.H. Breese, V.L.S. Fuh, E. Tang Xioasong, Opt. Expr. 16 (2008) 12757.
[15] N. Puttaraksa, M. Napari, L. Meriläinen, H.J. Whitlow, T. Sajavaara, L. Gilbert, Nucl. Instrum. Methods B306 (2013) 302.
[16] F. Watt, Xiao Chen, A. Baysic De Vera, C.N.B. Udalagama, Ren Minqin, J.A. van Kan, A.A. Bettiol, Nucl. Instrum. Methods B269 (2011) 2168–2174.
[17] D. Jun, P. Kruit, J. Vac. Sci. Technol. B29 (2011), 06F603-1–06F603-7.
[18] C.N.B. Udalagama, A.A. Bettiol, F. Watt, Phys. Rev. B 80 (2009) 224107.
[19] Y. Yao, P.S. Raman, J.A. van Kan, Microsyst. Technol. (2014), http://dx.doi.org/10.1007/s00542-014-2066-2.
[20] K. Ansari, J.A. van Kan, A.A. Bettiol, F. Watt, Appl. Phys. Lett. 85 (2004) 476–478, AIP Publishing LLC.
[21] N. Uchiya, Y. Furuta, H. Nishikawa, T. Watanabe, J. Haga, T. Satoh, M. Oikawa, Y. Ishii, T. Kamiya, Microsyst. Technol. 14 (2008) 1537–1540.
[22] Y. Tanabe, H. Nishikawa, Y. Seki, T. Satoh, Y. Ishii, T. Kamiya, T. Watanabe, A. Sekiguchi, Microelectron. Eng. 88 (2011) 2145–2148.
[23] S. Bolhuis, J.A. van Kan, F. Watt, Nucl. Instrum. Methods B267 (2009) 2302.
[24] F. Menzel, D. Spemann, S. Petriconi, J. Lenzner, T. Butz, Nucl. Instrum. Methods B250 (2006) 66.
[25] S. Yasin, D.G. Hasko, H. Ahmed, Microelectron. Eng. 61–62 (2002) 745.
[26] T. Andrea, M. Rothermel, T. Reinert, T. Koal, T. Butz, Nucl. Instrum. Methods B269 (2011) 2431.
[27] N. Puttaraksa, R. Norarat, M. Laitinen, T. Sajavaara, H.J. Whitlow, S. Singkarat, Nucl. Instrum. Methods B272 (2012) 162.
[28] J. van Erps, M. Vervaeke, H. Ottevaere, A. Hermanne, H. Thienpont, Nucl. Instrum. Methods B307 (2013) 243.
[29] T. Sakai, R. Yasuda, H. Likura, T. Nojima, M. Matsubayashi, W. Kada, M. Kohka, T. Satoh, T. Ohkubo, Y. Ishii, K. Takano, Nucl. Instrum. Methods B306 (2013) 299.
[30] I. Rajta, E. Baradács, A.A. Bettiol, I. Csige, K. Tőkési, L. Budai, Á.Z. Kiss, Nucl. Instrum. Methods B231 (2005) 384.
[31] E. Baradács, I. Csige, I. Rajta, Radiat. Measurements 43 (2008) 1354.
[32] MGT Mikroglas Technik AG, Mainz, Germany.
[33] M. Abraham, et al., MRS 2002 Fall Meeting Symposium H: Three-Dimensional Nanoengineered Assemblies, 2002.
[34] I. Rajta, M.I. Gomez, M.H. Abraham, Á.Z. Kiss, Nucl. Instrum. Methods B210 (2003) 260.
[35] W. Larisch, T. Koal, R. Werner, M. Hohlweg, T. Reinert, T. Butz, Nucl. Instrum. Methods B269 (2011) 2444.
[36] F. Watt, A.A. Bettiol, J.A. van Kan, E.J. Teo, M.B.H. Breese, Ion beam lithography and nanofabrication: a review, Int. J. Nanosci. 4 (3) (2005) 269–286, © World Scientific Publishing Company.
[37] J.A. van Kan, C. Zhang, P. Malar, J.R.C. van der Maarel, Biomicrofluidics 6 (2012), 036502-1.
[38] Y. Furuta, H. Nishikawa, T. Satoh, Y. Ishii, T. Kamiya, R. Nakao, S. Uchida, Microelectron. Eng. 86 (2009) 1396.
[39] F. Menzel, D. Spemann, T. Koal, T. Butz, Nucl. Instrum. Methods B269 (2011) 2427.
[40] F. van Delft, R. van de Laar, M. Verschuuren, E. Platzgummer, H. Loeschner, Microelectron. Eng. 87 (2010) 1062.
[41] Y.H. Wang, P. Malar, J.A. van Kan, Microsyst. Technol. (2014), http://dx.doi.org/10.1007/s00542-014-2070-6.
[42] J.A. van Kan, P.G. Shao, Y.H. Wang, P. Malar, Microsyst. Technol. 17 (2011) 1519.
[43] http://www.allresist.de/
[44] P. Malar, Zhao Jianhong, J.A. van Kan, Appl. Surf. Sci. 258 (2012) 4191.
[45] N.N. Liu, Shao Peige, S.R. Kulkarni, J. Zhao, J.A. van Kan, Key Eng. Mater. 447–448 (2010) 188–192.
[46] M. Chatzichristidi, I. Rajta, Th. Speliotis, E.S. Valamontes, D. Goustouridis, P. Argitis, I. Raptis, Microsyst. Technol. 14 (2008) 1423–1428.
[47] E. Valamontes, M. Chatzichristidi, N. Tsikrikas, D. Goustouridis, I. Raptis, C. Potiriadis, J.A. van Kan, F. Watt, Jpn. J. Appl. Phys. 47 (2008) 8600.
[48] M.D. Ynsa, P. Shao, S.R. Kulkarni, N.N. Liu, J.A. van Kan, Nucl. Instrum. Methods B269 (2011) 2409.
[49] J.A. van Kan, A.A. Bettiol, S.Y. Chiam, M.S.M. Saifullah, K.R.V. Subramanian, M.E. Welland, F. Watt, Nucl. Instrum. Methods B260 (2007) 460.
[50] B. O'Regan, M. Grätzel, Nature 353 (1991) 737.
[51] M. Yoshida, P.N. Prasad, Chem. Mater. 8 (1996) 235.
[52] S. Arakawa, K. Mogi, K. Kikuta, T. Yogo, S. Hirano, J. Am. Ceram. Soc. 82 (1999) 225.
[53] J. Livage, Mater. Res. Soc. Symp. Proc. 73 (1986) 717.
[54] M.S.M. Saifullah, K.R.V. Subramanian, E. Tapley, Dae-Joon Kang, M.E. Welland, M. Butler, Nano Lett. 3 (2003) 1587.
[55] K. Saito, H. Hayashi, H. Nishikawa, Nucl. Instrum. Methods B306 (2013) 284.
[56] R. Tsuchiya, H. Nishikawa, Trans. Mater. Res. Soc. Jpn. 36 (2011) 325.
[57] CSEM, Swiss Center for Electronics and Microtechnology, Neuchâtel, Switzerland (http://www.csem.ch).
[58] Y. Gonin, F. Munnik, F. Benninger, F. Dias, S. Mikhaílov, J. Vac. Sci. Technol. B22 (2004) 1982.
[59] E.J. Teo, M.H. Liu, M.B.H. Breese, E.P. Tavernier, A.A. Bettiol, D.J. Blackwood, F. Watt, Fabrication of silicon microstructures using a high energy ion beam, in: Proceedings of SPIE 5347, Micromachining Technology for Micro-Optics and Nano-Optics II, 2004, pp. 264–270.
[60] F. Watt, M.B.H. Breese, A.A. Bettiol, J.A. van Kan, Mater. Today 10 (2007) 20–29.
[61] S. Azimi, M.B.H. Breese, Z.Y. Dang, Y. Yan, Y.S. Ow, A.A. Bettiol, J. Micromech. Microeng. 22 (2012) 015015 (9 pp.).
[62] C. Liao, J.-S. Hsu, H.-M. Chang, J. Phys. Chem. Solids 69 (2008) 653.
[63] H. Kim, T.J. Lee, S. Kim, H. Lee, J. Nanosci. Nanotechnol. 11 (2011) 4378.
[64] Hu Jianmin, Wu Yiyong, Yang Dezhuang, He Shiyu, Zhang Zhongwei, Qian Yong, Zhang Mengyan, Nucl. Instrum. Methods B266 (2008) 3577.
[65] F. Menzel, D. Spemann, T. Butz, Nucl. Instrum. Methods B269 (2011) 2457.
[66] D. Diering, D. Spemann, J. Lenzner, St. Müller, T. Böntgen, H. von Wenckstern, Nucl. Instrum. Methods B306 (2013) 275.
[67] D.-W. Kim, D.-I. Kim, Y.-H. Huh, T.-K. Yang, Y.-S. Kim, M.-G. Ha, M.-S. Wond, K.-R. Kim, J.-H. Lee, Nucl. Instrum. Methods B266 (2008) 3263.
[68] M. Vujisic, K. Stankovic, P. Osmokrovic, IEEE (2009) 65–69, 978-1-4577-0493-2/09.
[69] A. Kitamura (Ogawa), T. Satoh, M. Koka, T. Kobayashi, T. Kamiya, Nucl. Instrum. Methods B307 (2013) 610.
[70] A. Kitamura (Ogawa), T. Satoh, M. Koka, T. Kobayashi, T. Kamiya, Nucl. Instrum. Methods B306 (2013) 288.
[71] S.Z. Szilasi, R. Huszank, A. Csik, C. Cserháti, I. Rajta, Nucl. Instrum. Methods B267 (2009) 2296.
[72] R. Huszank, S.Z. Szilasi, I. Rajta, A. Csik, Opt. Commun. 283 (2010) 176.
[73] M. Abesselam, D. Muller, M. Djebara, S. Ouichaoui, A.C. Chami, Nucl. Instrum. Methods B307 (2013) 635.
[74] D. Winston, B.M. Cord, B. Ming, D.C. Bell, W.F. DiNatale, L.A. Stern, A.E. Vladar, M.T. Postek, M.K. Mondol, J.K.W. Yang, K.K. Berggren, J. Vac. Sci. Technol. B 27 (2009) 2702.
[75] V. Sidorkin, E. van Veldhoven, E. van der Drift, P. Alkemade, H. Salemink, D. Maas, J. Vac. Sci. Technol. B 27 (2009) L18.
[76] C. Zhang, K. Jiang, F. Liu, P.S. Doyle, J.A. van Kan, J.R.C. van der Maarel, LOC 13 (2013) 2821.

[77] C. Zhang, A. Hernandez-Garcia, K. Jiang, Z. Gong, D. Guttula, S.Y. Ng, P.P. Malar, J.A. van Kan, Liang Dai, P.S. Doyle, R. de Vries, J.R.C. van der Maarel, Nucleic Acids Res. 41 (2013) e189.
[78] F. Menzel, D. Spemann, S. Petriconi, J. Lenzner, T. Butz, Nucl. Instrum. Methods B260 (2007) 419.
[79] N.N. Liu, P. Shao, S.R. Kulkarni, J.H. Zhao, J.A. van Kan, Key Eng. Mater. 447–448 (2010) 188.
[80] P. Mistry, M.I. Gomez, R.C. Smith, D. Thomson, G.W. Grime, R.P. Webb, R. Gwilliam, C. Jeynes, A. Cansell, M. Merchant, K.J. Kirkby, Nucl. Instrum. Methods B260 (2007) 437.